Investigating the Effects of Two Different Carbon Materials on the Sensitivity of an Electrochemical Impedimetric Lectin-Based Biosensor

Jianfang Qin, Haoyong Hao, Chenzhong Yao, Tiantian Jin, Haiying Yang[*]

Department of Chemistry, Yuncheng University, Yuncheng, 044300, PR China
[*]E-mail: haiyingyang79@hotmail.com

Carbon materials have proven to be promising materials in electrochemical biosensors. Here, the effect of two different carbon materials on the sensitivity of a label-free electrochemical impedimetric lectin-based biosensor was investigated. Graphene (G) and carbon nanospheres (CN-10) were individually used to fabricate a sensing surface with an incorporated electrodeposition of gold nanoparticles on a glassy carbon electrode. Lectin of Con A was covalently immobilized by a coassembly of 11-mercaptoundecanoic acid and dithiothreitol with carbodiimide chemistry. In a measurement of mannan (as the target model), the change in the interfacial electron transfer resistance of the biosensor was monitored using a redox couple of $Fe(CN)_6^{3-/4-}$, and this change was used to compare the effect of the two different carbon materials on the sensitivity of the biosensor. The results showed that G had a better performance than that of CN-10 under the conditions in this study. This work demonstrates that the use of G as an immobilization platform is a promising approach to designing impedimetric lectin-based biosensors with high sensitivity when compared to that of CN-10.

1. INTRODUCTION

Glycomics are becoming an important member of the 'omics' family now that glycosylation is the most frequent posttranslational modification of proteins and glycans involved in many physiological and pathological processes [1]. The major analytical tools in glycomics contain chromatographic techniques, mass spectrometry, capillary electrophoresis and especially lectin techniques. Lectin-based assays play an active role in glycans in many processes and are now regarded as a standard analytical tool in glycomics [2-8]. However, a typical lectin microarray experiment includes a fluorescent dye coupled either to lectin or to a glycan/sample to generate an analytical signal. This essential condition for having a label could lead to unwanted variability in labeling and biorecognition [6-8]. Therefore,

other methods of analysis working with a label-free mode of detection should be investigated. Electrochemistry is a powerful analytical method with different detection principles, and some are capable of working in a label-free mode of operation [9-11]. Because of its more sensitive analysis and simpler construction compared to that of other electrochemical sensing, electrochemical impedance spectroscopy (EIS) is usually employed in the fabrication of label-free biosensors.

The recent emergence of carbon-based materials, such as graphene (G), carbon nanofibers, carbon nanotubes, graphene oxide and carbon nanotubes (CN), have drawn much attention because of their high electrical conductivity, good mechanical flexibility, large surface areas and low cost [12-16]. The effect of these compounds on biosensor sensitivity should be addressed for the development of highly sensitive analytical methods. However, carbon materials tend to agglomerate due to strong π-π stacking and van der Waals interactions; thus, metal nanoparticles (NPs) have been proposed to separate sheets of carbon material [17-19]. It is well recognized that the dispersion of metal NPs on sheets of carbon materials also potentially provide a way of developing materials with novel properties. Gold nanoparticles (AuNPs) have been widely employed due to their benefits of good biocompatibility, high catalytic activity, and a high rate of electron transfer [20, 21].

Lectins, a group of proteins obtained from plants or animals, can specifically bind to carbohydrate moieties [1, 2]. Lectins are particularly interesting candidates as molecular recognition elements due to their ease of production and intrinsic stability. *Concanavalin* A (Con A), as a lectin extracted from *Canavalia ensiformis*, has been widely researched and used. On the basis of the interactions between lectins and glycoconjugates, a few biosensors have been designed because of the recognition ability of Con A towards carbohydrates [3-11].

The purpose of this work is to probe the effects of two carbon materials, graphene (G) and carbon nanospheres (CN-10), on the sensitivity of a label-free impedimetric lectin-based biosensor using mannan as a model target. As shown in Fig. 1, EIS biosensors were designed with the two carbon materials individually, and the detection processes were also illustrated. The biosensor was fabricated by casting G or CN-10 and Nafion onto a glassy carbon electrode (GCE). Nafion was used as a membrane matrix to improve the stability of the electrode and accelerate the ion exchange. The Au nanoparticles were electrodeposited onto the modified electrode surface. Third, a coassembly of MUA and DTT formed a binary membrane on the modified surface and the carboxyl group of MUA coupled with lectin through an amidation reaction. BSA was used as an interfacial layer to prevent nonspecific interactions. Once the biosensor interacted with the target, an increased EIS response was produced, which was directly proportional to the mannan concentration. The analytical performance of the G- or CN-10-based biosensor for mannan was compared.
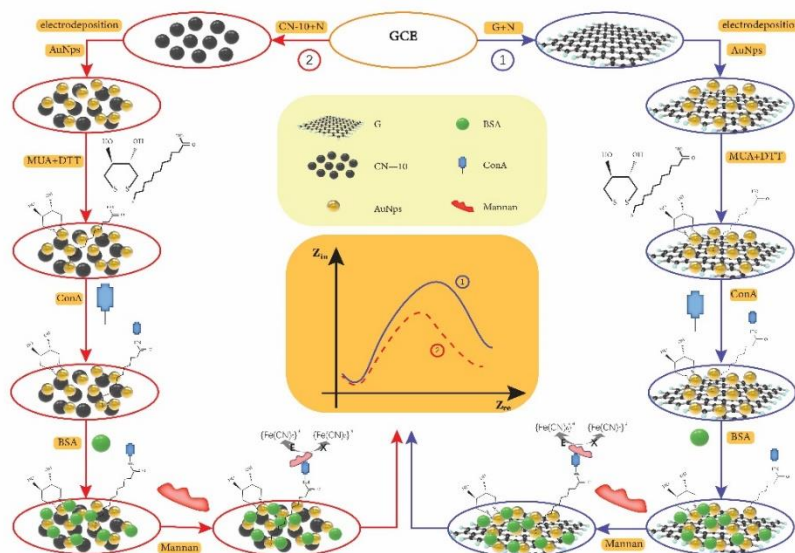
Figure 1. Schematic of the comparative study on the effects of graphene (G) and carbon nanospheres (CN-10) on the performance of an impedimetric biosensor using mannan as a model target.

2. EXPERIMENTAL

2.1. Chemicals and materials

Graphene (G) and carbon nanospheres (CN-10) were purchased from Nanjing Xianfeng Nano-Materials Technology Co. Ltd. (Nanjing, China). Concanavalin A (ConA) from *Canvalia ensiformis* type IV (M.W.=104 kDa), 11-mercapto-1-undecanoic acid (MUA), dithiothreitol (DTT), N-acetyl-glucosamine (GlcNAc), glucose, mannose, galactose, N-(3-dimethylaminopropyl)-N-ethylcarbodiimide hydrochloride (EDC), N-hydroxysuccinimide (NHS) and Nafion (5 wt%) were supplied from Sigma-Aldrich (St. Louis, USA). HAuCl$_4$, potassium ferricyanide (K$_3$[Fe(CN)$_6$]) and potassium ferrocyanide (K$_4$[Fe(CN)$_6$]), MnCl$_2$, CaCl$_2$, potassium chloride (KCl), and N,N-dimethylformamide (DMF) were obtained from Sinopharm Chemical Reagent Co. Ltd. (Shanghai, China). Bovine serum albumin (BSA) was purchased from Shanghai Sangon Biological Engineering Technology (China). All reagents were used as supplied without further purification.

Phosphate buffer saline (PBS, 10 mM, pH 7.4) was used as a Con A immobilization buffer and washing buffer. PBS (10 mM) containing CaCl$_2$ (1 mM) and MnCl$_2$ (1 mM) were used as a binding buffer. All carbohydrate solutions were prepared with the binding buffer. Ultra-pure water (18.2 MΩ cm) was used in all experiments.

2.2. Apparatus and measurements

The morphology of the modified electrodes was characterized by scanning electron microscopy (SEM Hitachi S-4800 microscope, Japan). A CHI-660 electrochemical workstation (Chenhua

Instruments Co. Shanghai, China) was utilized for the electrochemical measurements. All electrochemical experiments were carried out using a traditional three-electrode system with a fabricated biosensor or a glassy carbon electrode (GCE) as the working electrode, a platinum wire as the counter electrode, and an Ag/AgCl (sat. KCl) as the reference electrode. All potentials are reported with regard to the reference electrode.

2.3 Fabrication of the electrochemical Con A-based biosensor

Graphene (G, 2 mg) was dispersed in 2 mL DMF. Nafion (0.5 wt%) was added to it and then placed under mild ultrasonication for 2 h to form homogeneous suspensions. Therefore, a dispersion containing G (1 g/L) and Nafion (0.5 wt%) was obtained at a ratio of 1:1 (v/v). The glassy carbon electrode (GCE) was polished using an aqueous alumina slurry (0.05 µm). Finally, the electrode was washed thoroughly with ultra-pure water to obtain a clean surface.

A 5 µL suspension of G and Nafion was cast on a GCE and dried at room temperature to obtain the G/Nafion/GCE. Next, the Au nanoparticles were electrodeposited onto the prefabricated electrode in a mixed solution of 3.0 mM $HAuCl_4$ and 0.5 M H_2SO_4 at a constant potential of -0.2 V for 400 s. The as-prepared electrode was denoted as AuNPs/G/Nafion/GCE. The electrode was rinsed with water. Then, a 10 µL mixture of 1 µM MUA and 10 µM DTT was dropped onto the AuNPs/G/Nafion/GCE surface and placed in a refrigerator (4 °C) for 14 h to obtain the MUA/AuNPs/G/Nafion/GCE. The as-prepared electrode was activated in 100 µL of freshly prepared solution containing 2 g/L EDC and 5 g/L NHS for 30 min to activate the carboxylic groups on MUA. Then, the activated electrode was immersed in 100 µL of 1 g/L Con A solution for 1 h. The ConA/MUA/AuNPs/G/Nafion/GCE was immersed in 100 µL of 1% BSA for 30 min to inhibit nonspecific interactions and then it the electrode was rinsed thoroughly to remove any adsorbed components. The ConA-based biosensor (ConA/AuNPs/G/Nafion/GCE) was obtained and stored at 4 °C in PBS (pH 7.4). The same processes were performed to prepare CN-10-based biosensors except G was replaced with CN-10 .

2.4. Electrochemical measurement

The biosensors were immersed in 100 µL PBS containing different concentrations of mannan for 60 min and then washed. Electrochemical measurements were performed in 10 mM PBS containing 5 mM $[Fe(CN)_6]^{3-/4-}$ with a 5 mV sinusoidal excitation amplitude. The EIS was recorded at 0.2 V (*vs.* Ag/AgCl) within a frequency range from 100 kHz to 0.1 Hz and a sampling rate of 12 points per decade. A Randles equivalent circuit was selected for fitting of the measured EIS results. The concentration of mannan was quantified by an increase in the electron transfer $\Delta R_{et} = R_{et.i} - R_{et.0}$, where $R_{et.0}$ and $R_{et.i}$ are the electron transfer resistance values before and after incubation with carbohydrates, respectively.

Cyclic voltammetry (CV) was used to monitor the fabrication process of the biosensor. All the voltammograms were recorded from -0.2 V to 0.6 V at a scan rate of 0.1 V/s. All electrochemical experiments were performed at room temperature (25 ± 1 °C).

3. RESULTS AND DISCUSSION

3.1 Characterization of Con A-based biosensor

As shown in Fig. 2a and Fig. 3a, the characterization results of the different modified electrodes by cyclic voltammetry (CV) experiments, using $[Fe(CN)_6]^{3-/4-}$ as a redox indicator, decreased with the step-by-step fabrication process except for after the electrodeposition of AuNPs because it could accelerate the electron transfer between the electrode and the modified materials. When testing for the model target mannan, the smaller current obtained might be attributed to a blocking effect of mannan toward the electron transfer. A similar current change trend was observed for the two carbon materials, G and CN-10, demonstrating that they had a similar effect on the fabrication biosensor.
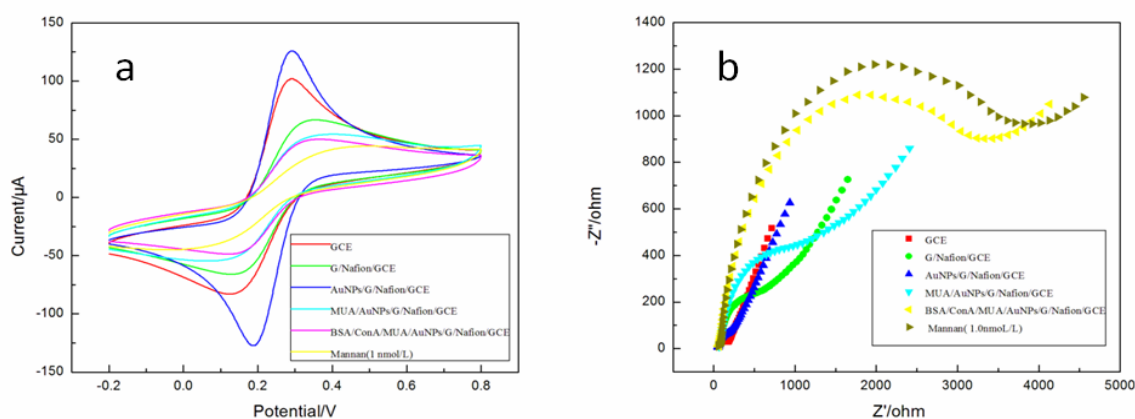
Figure 2. (a) CV of graphene (G)-modified electrodes from -0.2 V to 0.6 V at a scan rate of 0.1 V/s. (b) Nyquist plots of graphene (G)-modified electrodes within a frequency range from 100 kHz to 0.1 Hz. All experiments were performed in 10 mM PBS containing 5 mM $[Fe(CN)_6]^{3-/4-}$ and 0.1 M KCl.
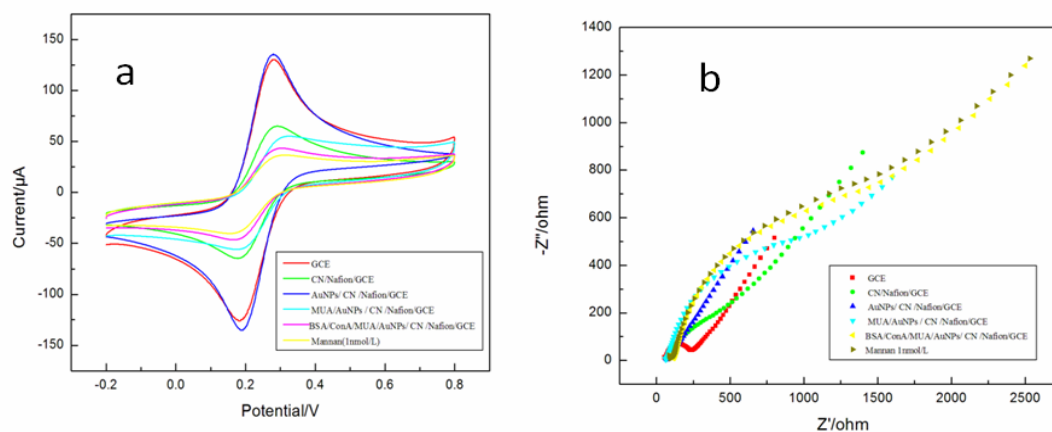
Figure 3. (a) CV of carbon nanosphere (CN-10)-modified electrodes from -0.2 V to 0.6 V at a scan rate of 0.1 V/s. (b) Nyquist plots of carbon nanosphere (CN-10)-modified electrodes within a frequency range from 100 kHz to 0.1 Hz. All experiments were performed in 10 mM PBS containing 5 mM $[Fe(CN)_6]^{3-/4-}$ and 0.1 M KCl.

To obtain detailed information, electrochemical impedance spectroscopy (EIS), as one of the most powerful tools, was used to characterize the interfacial properties of the biosensor fabrication process and binding process. Nyquist plots were generated when the GCE was subjected to the step-by-step modification process using $[Fe(CN)_6]^{4-/3-}$ as the redox indicator. The change in the electron transfer resistance (ΔR_{et}) was used as the signal.

As shown in Fig. 2b, for the G-modified electrode, the electrochemical response was a nearly straight line and showed a very fast electron transfer process with a bare electrode. The G/Nafion/GCE showed an increase in the charge transfer resistance. Nafion film acted as a blocking layer that obstructed the diffusion of $[Fe(CN)_6]^{3-/4-}$ toward the electrode surface owing to its permeability to cations [22], this led to an increase of the semicircle diameter. Then, the AuNPs were electrodeposited on the surface of the G/Nafion/GCE. The ΔR_{et} value exhibited an obvious reduction to 90 Ω, which might be attributed to the AuNPs, which could accelerate the electron transfer [23, 24]. The effect of the AuNPs was checked in detail later. When MUA+DTT were coassembled on the AuNPs/G/Nafion/GCE, this step led to a dramatic increase in the R_{et} value from 90 to 1234 Ω, which contributed to the formation of highly ordered and oriented insulating films blocking the penetration of redox species toward the electrode surface [25]. After Con A was covalently combined with the carboxyl group of MUA using carbodiimide chemistry, the R_{et} value greatly increased to 3266 Ω. After blocking with BSA, the R_{et} value increased from 3266 to 5680 Ω. Finally, the binding of mannan with the lectin interface continually increased the R_{et} value. A similar R_{et} change trend in the R_{et} value was observed for the CN-10 modified biosensor, while a poor semicircle showed the low electron transfer property of CN-10. The above results were in good agreement with the results obtained from CV.

The increases in the R_{et} value were mainly attributed to the insulating nature of Con A and BSA obstructing the redox probe to the electrode surface. After the biosensor was bound with 1 nM mannan, R_{et} increased to 7421 Ω, which indicated that G and AuNPs, MUA + DTT, Con A, BSA, and mannan have been successively assembled onto the GCE in sequence and that the as-designed electrochemical biosensor could work successfully. The biosensor modified with G showed a larger value change in ΔR_{et} compared with that based on CN-10, which indicated that the biosensor with G possessed higher sensitivity.

To illustrate the effect of AuNPs in this study, the effective surface area of the modified electrodes could be estimated based on the Randles-Sevcik equation [26, 27].

$$I_{pc} = 2.69 \times 10^5 n^{3/2} A D^{1/2} C v^{1/2} \qquad (1)$$

where I_{pc} is the reduction peak current (A), n is the electron transfer number, A is the effective electrode area (cm^2), D is the diffusion coefficient of $K_3[Fe(CN)_6]$ (cm^2/s), C is the concentration of $K_3[Fe(CN)_6]$ (M) and v is the scan rate (V/s). By analyzing the reduction peak current with scan rate, the average effective electrode area of GCE, G/Nafion/GCE and AuNPs/G/Nafion/GCE were estimated to be 1.22×10^{-1}, 7.03×10^{-2} and 1.41×10^{-1} cm^2, respectively. The AuNPs/G/Nafion/GCE had the largest apparent surface area and the smallest charge transfer resistance value. The results demonstrated that introducing AuNPs in this study could increase the electrode surface and accelerate the electron transfer. Additionally, AuNPs might overcome the shortcomings of G, namely, its tendency to agglomerate or restack due to strong π-π stacking and van der Waals interactions, and showed the synergistic effect between G and AuNPs for improvement of the biosensor interfacial conductivity [28].

3.2 Analytical performance of the biosensor

The quantitative behavior of the G-modified biosensor was performed by measuring the dependence of ΔR_{et} on the concentration of mannan. Fig. 4 shows the EIS responses from the biosensor with different concentrations of mannan. The increased ΔR_{et} value was logarithmically proportional to the concentration of mannan in the range from 1.0×10^{-9} M to 5.0×10^{-7} M, and increased from 3063 to 35090 Ω. The linear regression equation was $\Delta R_{et} = 12120 \lg C + 110411$, with a regression coefficient of 0.9863. The detection limit was calculated to be 0.03 nM based on a signal-to-noise ratio of 3σ, where σ was the standard deviation of the signals obtained in 7 parallel EIS measurements using a blank solution.

To probe the different effects of the two materials on the sensitivity of the biosensors, a control experiment using CN-10 as the modified material was conducted. Fig. 5 shows the EIS responses from the biosensor. The increased EIS values were logarithmically proportional to the concentration of mannan with a linear regression equation of $\Delta R_{et} = 810 \lg C + 10569$ in the range of 1.0×10^{-9} M to 5.0×10^{-7} M. The correlation coefficient was 0.9528, and the detection limit was 0.08 nM. For a quantitative comparison, calibration curves were drawn for the two different biosensors, and it was clear that the signals were higher for the G-based biosensor. The sensitivity of the present study (12120 $\Omega/\lg(nM)$) based on the G-modified biosensor was approximately 15-fold higher than that obtained from the CN-10-modified biosensor (810 $\Omega/\lg(nM)$), which was attributed to the enhancement effect of G. Thus, the results indicated the relatively higher sensitivity obtained using G as the sensing surface for fabricating the biosensor.
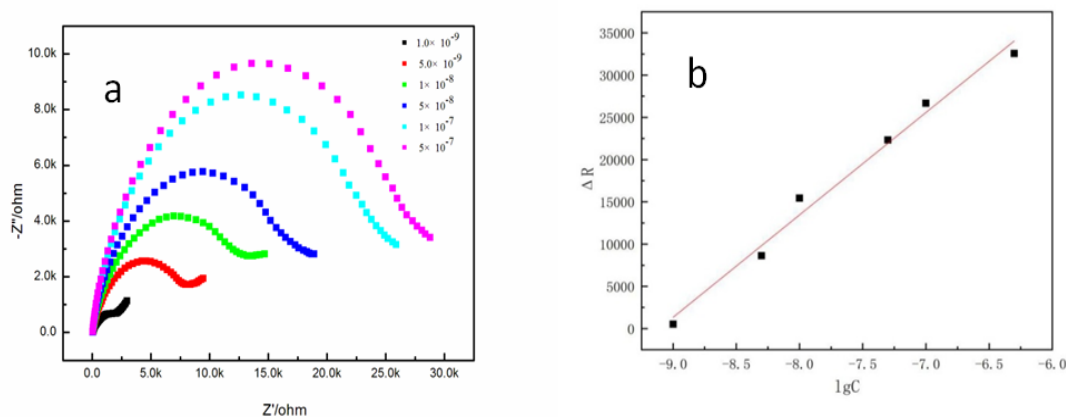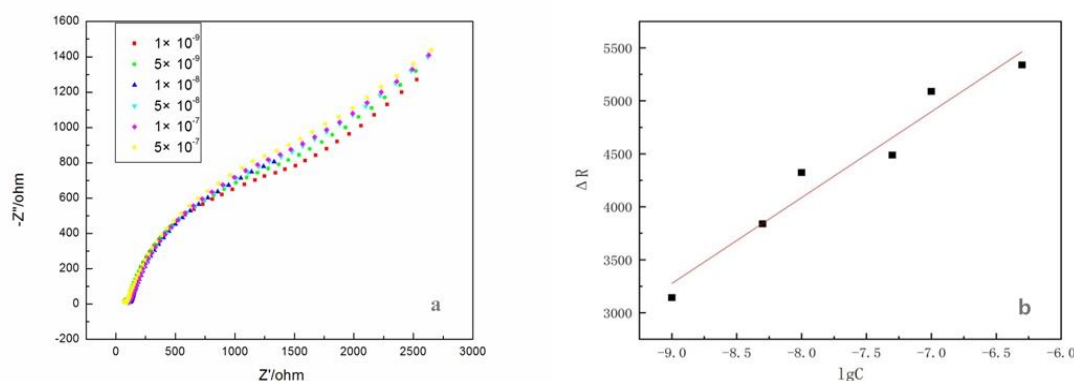

Figure 4. (a) Nyquist plots of the BSA/ConA/MUA/AuNPs/G/Nafion/GCE immersed in a mannan concentration range of 1.0×10^{-9} mol/L to 5.0×10^{-7} mol/L. (b) The linear relationship between ΔR_{et} and the different concentrations of mannan. $\Delta R_{et} = R_{et,i} - R_{et,0}$, where $R_{et,0}$ and $R_{et,i}$ are the electron transfer resistance values before and after incubation with mannan.

The electrochemical process of the G-modified biosensor was also checked, and it was found that the anodic peak potential of the AuNPs/G/Nafion/GCE shifted positively with a scan rate increase, while the cathodic peak potential shifted negatively. Meanwhile, the peak current increased with a scan rate from 100 mV/s to 650 mV/s, and the anodic and cathodic peak currents were proportional to the square root of the scan rate. The following equations were obtained:

$$I_{p,a}(A) = 0.1509v^{1/2}(V/s) + 1.8084 \ (R^2 = 0.9808) \quad (2)$$
$$I_{p,c}(A) = -0.2084v^{1/2}(V/s) - 1.6489 \ (R^2 = 0.9872) \quad (3)$$

Figure 5. (A) Nyquist plots of the CN-10-based biosensor immersed in a mannan concentration range of 1.0×10^{-9} mol/L to 5.0×10^{-7} mol/L. (B) The linear relationship between ΔR_{et} and the different concentrations of mannan. $\Delta R_{et} = R_{et,i} - R_{et,0}$, where $R_{et,0}$ and $R_{et,i}$ are the electron transfer resistance values before and after incubation with mannan.

The results indicated that the electrochemical process was a diffusion-controlled process. Simultaneously, the linear relationships between the peak potential (E_p) and the Napierian logarithm of the scan rate (lnv) for both the cathodic and anodic peaks were also obtained.

$$E_{p,a}(V) = -0.0211\ln v(V/s) + 0.2157 \ (R^2 = 0.9873) \quad (4)$$

$$E_{p,c}(V) = 0.0224\ln v(V/s) + 0.1677 \ (R^2 = 0.9732) \quad (5)$$

According to Laviron [29],

$$E_{p,a} = E^\theta + \frac{RT}{\alpha nF}\ln k^\theta + \frac{RT}{\alpha nF}\ln v \quad (6)$$

where α is the transfer coefficient, k^θ is the electrochemical rate constant, n is the number of electrons transferred in the rate determining step, v is the scan rate, E^θ is the formal potential, and R, T and F have their usual meanings. The value of α was calculated to be 1.1.

Additionally, the fabrication of biosensors was also characterized by SEM. The images of bare GCE, G/Nafion/GCE and AuNPs/G/Nafion/GCE are shown in Fig. 6. From Fig. 6a, the surface of the bare GCE was smooth, while the surface of the G and Nafion-modified GCE was nonuniform. The G sheets were covered on the surface of the GCE (Fig. 6b). As shown in Fig. 6c and Fig. 6d, Au nanoparticles with flower-like structures were clearly observed on the surface of the electrodes.

The reproducibility of the biosensor for binding mannan was assessed. The RSD for five biosensors were 6.9% and 6.2% at mannan concentrations of 1 nM and 10 nM, respectively. The results indicated that the reproducibility was acceptable. The EIS value of the biosensor to 1 nM mannan lost approximately 9.5% and 12.4% of its original response after 10 days and 20 days, respectively. Thus, the long-term storage of the fabricated biosensor needs ongoing research.

To assess the selectivity of the biosensor, a series of carbohydrates were tested (Fig. 7a) by examining the R_{et} after incubation with carbohydrates, including a specific binding carbohydrate and nonspecific carbohydrates for Con A. The measured $\Delta R_{et}/R_{et,0}$ value was used to check the selectivity of the biosensor. The selectivity was 4.03 for mannan and 0.06-0.22 for the other carbohydrates. All these results showed that the EIS biosensor possessed satisfactory selectivity due to the incubation ability of Con A.
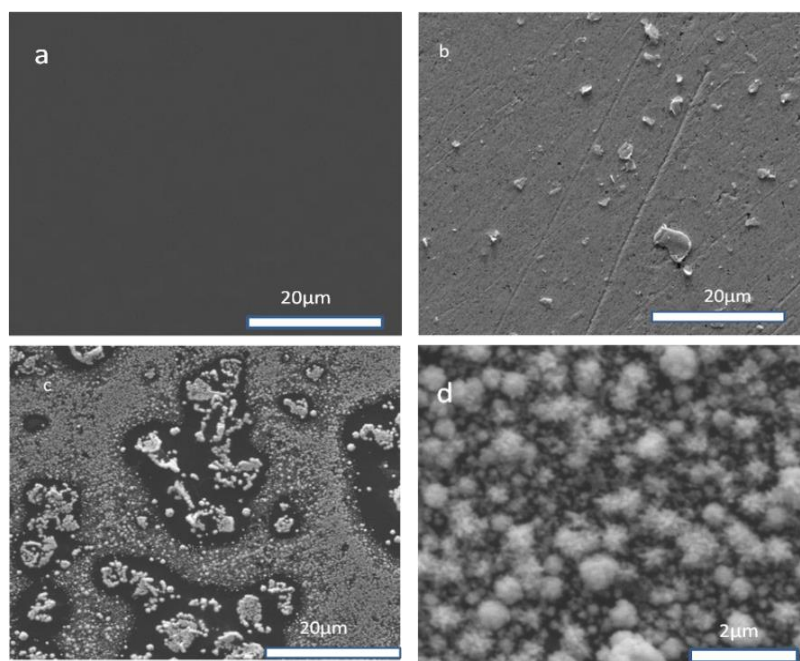
Figure 6. SEMs of the different modified electrode surfaces: (a) GCE, (b) G/Nafion/GCE, (c) AuNPs/G/Nafion/GCE, and (d) a magnification of (c).

The binding ability between Con A immobilized in the G-modified biosensor and mannan was also checked using a proposed EIS method [39], and a binding constant of $5.9 \times 10^9 \, M^{-1}$ was obtained from Fig. 7b. This value was consistent with $5.3 \times 10^9 \, M^{-1}$ by SPR for yeast mannan and Con A [40] and was slightly lower than $5.2 \times 10^{10} \, M^{-1}$ as determined by the ECL method for Con A immobilized on SWCNTs [8], and was also compared with other reusutls published, as shown in Table 1. The large binding constant value obtained by the G-modified biosensor indicated that the binding strength between mannan and Con A was strong [3-11].

Table 1. Comparison of the proposed method with some reported lectin-based biosensors

Detection technique	Assay principle	Lectin	carbohydrate	Associated constant, Ka (M^{-1})	Refs
EIS	MUA and DTT mixed SAM	Con A	mannan	3.8×10^7	[9]
EIS	carbohydrate analogues immobilized by click" reaction	*Lens culinaris*	mannose	$2.63 \pm 0.5 \times 10^6$	[10]

		at BDDE	lectin		
EIS	Multi-wall carbon nanotube-polyaniline	Con A	d-glucose	Linear range 3.3 pM-9.3 nM	[11]
ECL	SWCNT coated on screen-printed carbon electrode	Con A	mannan	5.2×10^{10}	[8]
SPR	polyethylene glycol alkanethiol mixed SAM	Con A	*Yeast mannan*	5.3×10^{9}	[3]
SPR	Various degrees of oxidation *mannan on* gold surface	Con A	yeast *mannan from Saccharomyces cerevisiae*	Kd 5.2×10^{-8} M	[4]
QCM	polystyrene-coated quartz crystals	Con A	*Yeast* mannan	Kd 4.0×10^{-7} M	[5]
Fluorescence	Chip-based assay	Con A	Man9	Kd 73 nM	[6]
Fluorescence	Array-based assay	Con A	Man 6	Kd 49±29 nM	[7]
EIS	Graphene-AuNPs modified sensor surface	Con A	mannan	5.9×10^{9}	This work

Note: EIS means electrochemical impedance spectroscopy; ECL means electrogenerated chemiluminescence, SPR means surface plasmon resonance, QCM means quartz crystal microbalance. SAM means self-assemble membrane. K_D means dissociation constant, K_a means association constant.
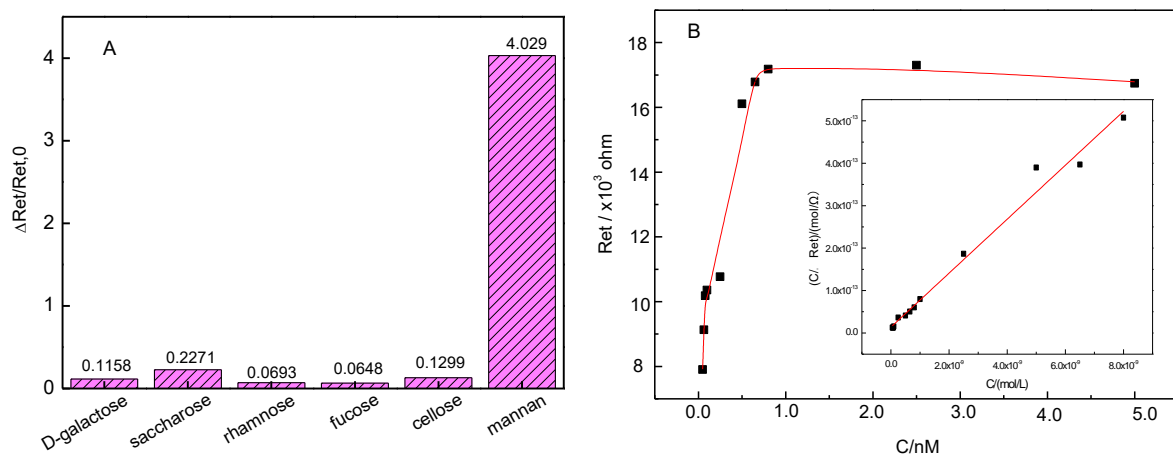
Figure 7. (A) Graph of $\Delta R_{et}/R_{et,0}$ for the biosensor incubated with 1 nM of different carbohydrates. (B) Langmuir isotherms obtained after the biosensor interacted with mannan from 0.05 nM to 8.0 nM. The nonlinear regression between ΔR_{et} and C_{mannan} and the insert shows the linear regression between $C_{mannan}/\Delta R_{et}$ and C_{mannan}.

4. CONCLUSION

In conclusion, the effect of two different carbon materials (graphene and carbon nanospheres) on the sensitivity of an EIS lectin-based biosensor was investigated using an interaction between Con A and mannan as a model. An electrodeposition of AuNPs was also used to help fabricate the biosensor, and its function was also checked, showing that the incorporation of AuNPs increased the effective surface of the modified electrode and increased the electron transfer. By comparing the analytical

performance of the two biosensors based on G and CN-10, the results showed that G had better performance than CN-10 for the determination of mannan under the conditions in this study. This work demonstrates that the use of G as an immobilization platform is a promising approach to designing impedimetric lectin-based biosensors with high sensitivity when compared to that of CN-10.

References

1. D. Kolarich, B. Lepenies and P.H. Seeberger, *Curr. Opin. Chem. Biol.*, 8 (2011) 1.
2. J. F. Rakus, L. K. Mahal and L. K. Annu, *Rev. Anal. Chem.*, 4 (2011) 367.
3. M. Jana, S. D. Estera, C. Jenny and D. Bengt, *J. Biochem. Biophys. Methods*, 60 (2004) 163.
4. D. Mislovicova, J. Masarova, J. Syvitel, R. Mendichi, L. Syoltes, P. Gemeiner and B. Danielsson, *Bioconjugate Chem.*, 13 (2002) 136.
5. Z. Pei, H. Anderson, T. Aastrup and O. Ramstrom, *Biosens, Bioelectron.*, 21(2005) 60.
6. P. H. Liang, S. K. Wang and C. H. Wong, *J. Am. Chem. Soc.*, 129 (2007) 11177.
7. Y. Zhang, Q. Li, L. G. Rodriguez and J. C. Gildersleeve, *J. Am. Chem. Soc.*, 132 (2010) 9653.
8. H. Y. Yang, Y. Q. Wang, H. L. Qi, Q. Gao and C. X. Zhang, *Biosens, Bioelectron.*, 35(2012) 376.
9. H. Y. Yang, H. Zhou, H. Hao, Q. Gong and K. Nie. *Sens. Actuator*, 229 (2016) 297.
10. S. Szunerits, J. Niedziołka-Jonsson, R. Boukherrou, P. Woisel, J. Baumann and A. Siriwarden, *Anal. Chem.*, 82 (2010) 8203.
11. F. Hu, S. Chen, C. Wang, R. Yuan, Y. Xiang and C. Wang, *Biosens, Bioelectron.*, 34 (2012) 202.
12. M. D. Stoller, S. Park, Y. Zhu, J. An and R.S. Ruoff, *Nano Lett.*, 8 (2008) 3498.
13. S. Stankovich, D. A. Dikin, G. H. Dommett, K.M. Kohlhaas, E. J. Zimney, E. A. Stach, R. D. Piner, S. T. Nguyen and R. S. Ruoff, *Nature*, 442 (2006) 282
14. A. Fasolino, J. H. Los and M. I. Katsnelson, *Nat. Mater.*, 6 (2007) 858.
15. R. Pasricha, S. Gupta and A. K.Srivastava, *Small,* 20 (2009) 2253.
16. H. Hu, X. Wang, J. Wang, L. Wan, F. Liu, H. Zheng, R. Chen and C. Xu, *Chem. Phys. Lett.,* 484 (2010) 247.
17. Y. Si and E. T. Samulski, *Chem. Mater.*, 20 (2008) 6792.
18. R. Pasricha, S. Gupta and A. K. Srivastava, *Small*, 5 (2009) 2253.
19. Y. H. Lu, M. Zhou, C. Zhang and Y. P. Feng, *J. Phys. Chem.* C, 113 (2009) 20156.
20. K.S. Novoselov, A.K. Geim, S.V. Morozov, D. Jiang, Y. Zhang, S.V. Dubonos.V. Grigorieva and A.A. Firsov, *Science,* 306 (2004) 666.
21. Y. Qi, J. He, F. R. Xiu, X. Yu, Y. Li, Y. Lu, X. Gao, Z. Song and B. Li, *Spectrosc. Spectrochim. Acta.* A. 216 (2019) 310.
22. E. Engin, C. H. Elikkan and Nevin Erka. *Sens. Actuators* B 224 (2016) 170.
23. W. J. Li, R.Yuan, Y. Q. Chai, H. A. Zhong and Y.Wang, *Electrochim. Acta*, 56 (2011) 4203.
24. K. Lebed, A. J. Kulik, L. Forró and M. Lekka, *J. Colloid Interfaces Sci.*, 299 (2006) 41.
25. Szunerits, S. Niedziŏłka-Jonsson, J. Boukherroub, R. Woisel, P. Baumann and J. S. Siriwardena, *Anal. Chem.*, 82 (2010) 8203.
26. S. Rengaraj, A. Cruz-Izquierdo, L. Janet Scott and M. Di Lorenzo, *Sens. Actuators* B, 265 (2018) 50.
27. W. Sun, X. Qi , Y. Chen , S. Liu and H. Gao, *Talanta*, 87 (2011) 106.
28. H. Yu, X. Feng, X. Chen, Sh. Wang and J. Jin. *J. Electroanal. Chem.*, 801 (2017) 488.

29. E. Laviron, *J. Electroanal. Chem.*, 52 (1974) 355.